New Journal of Physics
An Institute of Physics and Deutsche Physikalische Gesellschaft Journal

# Excitation waves in reaction–diffusion media with non-monotonic dispersion relations

**Chad T Hamik and Oliver Steinbock**[1]
Department of Chemistry and Biochemistry, Florida State University, Tallahassee, FL 32306-4390, USA
E-mail: steinbck@chem.fsu.edu

*New Journal of Physics* **5** (2003) 58.1–58.12 (http://www.njp.org/)
Received 22 January 2003
Published 6 June 2003

**Abstract.** We report results on chemical wave propagation obtained from experiments with a modified Belousov–Zhabotinsky reaction. Under pseudo-one-dimensional reaction conditions, excitation pulses either form closely stacked, stable wavepackets or merge with a slow leading pulse in front-to-back collisions. Moreover, wave stacking can involve the cascading formation of metastable clusters. These phenomena are due to anomalous dispersion relations in which the derivative of the pulse speed with respect to wavelength can involve negative values. Wave stacking and merging are also observed in thin reaction layers where they affect the evolution of target patterns. Additional results on the concentration dependences of the overall dynamics and pulse speeds are presented.

## Contents



[1] Author to whom correspondence should be addressed.


PII: S1367-2630(03)58606-2

## 1. Introduction

Reaction systems far from thermodynamic equilibrium can form a fascinating wealth of spatio-temporal patterns [1]. These dissipative structures often result from autocatalytic processes that are spatially coupled by transport phenomena such as diffusion or electric currents. They encompass stationary Turing patterns as well as travelling waves, both of which have attracted considerable interest in physics, chemistry and biology [2]–[6]. Of particular importance are wave patterns in excitable systems in which a local perturbation must exceed a certain threshold value to trigger a propagating chain of excitation events [7]. In response to a super-threshold perturbation, the system undergoes a large amplitude change before it relaxes into its dynamically stable rest state. Important examples for this type of behaviour are found in a variety of living systems including calcium waves in single cells [8], morphogenetic waves in aggregating colonies of micro-organisms [9] and propagating action potentials in cardiac and neuronal tissue [10, 11].

Non-biological systems, such as the Belousov–Zhabotinsky (BZ) reaction, provide ideal models for the quantitative experimental analysis of the generic spatio-temporal phenomena in excitable reaction–diffusion systems [1, 12]. Many of these phenomena can be discussed in terms of a set of two coupled reaction–diffusion equations governing the evolution of the concentration distribution of a fast activator and a slow control species [13]. In the closed BZ reaction, the local dynamics can be monostable, excitable or oscillatory. Excitable BZ systems show solitary pulses that propagate with a constant velocity that depends on the diffusion constant of the activator species ($HBrO_2$) and the rate constant of the autocatalytic reaction step [14]. The dynamics of wave trains is more complex because the distance between the pulse and its predecessor plays an important role. If this distance is large, the medium in front of the pulse is fully recovered and the propagation velocity is essentially identical to a solitary pulse. In the case of short distances, however, the relaxation dynamics of the system has a profound impact on the dynamics of trailing pulses [15, 16]. The resulting wavelength–velocity dependence is referred to as the system's dispersion relation. Numerical studies typically determine these dispersion relations by simulating a single excitation pulse within a circular, one-dimensional medium [16, 17]. This configuration mimics the dynamics of an infinite wave train but obviously does not allow for variations of the, possibly unstable, interpulse distances.

Most experimental systems obey a simple dispersion relation in which the pulse velocity, $c$, increases monotonically with increasing wavelength, $\lambda$, to saturate at the speed of the solitary pulse [15, 18]. For this normal dispersion relation, the derivative $\mathrm{d}c/\mathrm{d}\lambda$ is positive for all wavelengths. Additionally, excitable systems have a minimal wavelength below which no wave trains exist. These most common features of dispersion relations have been observed in numerous experimental systems including electrodissolution processes [19] and aggregating slime mould colonies [20]. Moreover, Flesselles *et al* [21] analysed dispersion data from chemical waves in the BZ reaction and found that the propagation velocities can be described as the hyperbolic tangent of the normalized periods. This finding is characteristic of media with simple exponential relaxation.

Despite the abundance of normal dispersion in various chemical and biological systems, even simple reaction–diffusion models can give rise to non-monotonic dispersion curves [22]–[26]. This behaviour can be understood by a simple linear stability consideration. In a typical excitable medium, the steady state is a stable node that becomes unstable as the system bifurcates to oscillatory dynamics. Near the Hopf bifurcation point, the real parts of the eigenvalues vanish

and the stable node becomes a stable spiral. Consequently, excitation pulses can be followed by non-monotonic relaxation processes, which then give rise to an overshoot or ripples in the dispersion relation [27, 28]. Notice that a rigorous description of this anomalous dispersion requires analysis of the full reaction–diffusion system and its wave solutions in co-moving coordinates.

Anomalous dispersion relations are known to exist in neuronal systems [29] and possibly in the cellular slime mould *Dictyostelium discoideum* [30]. Moreover, recent studies on the reduction of NO with CO on Pt(100) surfaces [31] and a modified BZ reaction [32]–[34] have revealed anomalous dispersion in non-biological reaction media. In this paper, we give a summary of some pertinent findings obtained from experiments with the latter reaction and analyse the evolution of two-dimensional wave patterns.

## 2. Materials and methods

All of the reagents employed in this study are of the highest grade commercially available and used without further purification. Stock solutions of sodium bromate ($NaBrO_3$, Fluka) and 1,4-cyclohexanedione ($C_6H_8(=O)_2$, Aldrich) are prepared in nanopure water obtained from a microfiltration system (Barnstead EASYpure UV, 18 MΩ cm). Ferroin solution ($[Fe(phen)_3]^{2+}$, Fluka, puriss. p.a.; 25 mM) and sulfuric acid ($H_2SO_4$, Fisher) are used without further preparation. The stock solutions are mixed in the following order: water, sulfuric acid, 1,4-CHD, sodium bromate and lastly ferroin. The temperature of the stock solutions and the reaction system is kept constant at 25 °C.

All of the experiments described in section 3.1 were carried out in glass capillary tubes. The inner diameter and the length of the capillaries are 1.1 and 75 mm, respectively. In contrast to the classical BZ reaction that employs malonic acid ($H_2C(COOH)_2$) as its organic substrate, the CHD–BZ reaction does not generate gaseous products and the spatial homogeneity of our experimental system is therefore not compromised by bubbles [35]—[37].

All experiments described in section 3.2 involve thin layers of the aqueous reaction medium that are created by confining the solution between two flat glass plates. The typical height of the layer is 0.5 mm. These pseudo-two-dimensional reaction conditions suppress the undesired loss of bromine from the liquid into the gas phase and minimize hydrodynamic perturbations.

The samples are illuminated with diffusive white light to avoid reflection from the glass surfaces of the batch reactors. The optical contrast arises from the profoundly different absorption spectra of the redox couple ferroin (red, reduced)/ferriin (blue, oxidized) [12, 14]. All experiments are monitored using an imaging system that consists of a PC-based frame grabber board (data translation; $640 \times 480$ pixels resolution with 8 bit/pixel) and a monochrome charged-coupled device camera (COHU 2122). The frame grabber board is controlled by commercial software (HLImage++97).

The data collection is started towards the end of the induction period. At this time, the reaction system switches from the spatially homogeneous oxidized state into the reduced (excitable) state. Notice that the induction time in the CHD–BZ system is rather long and varies with the initial concentrations around 30 min.

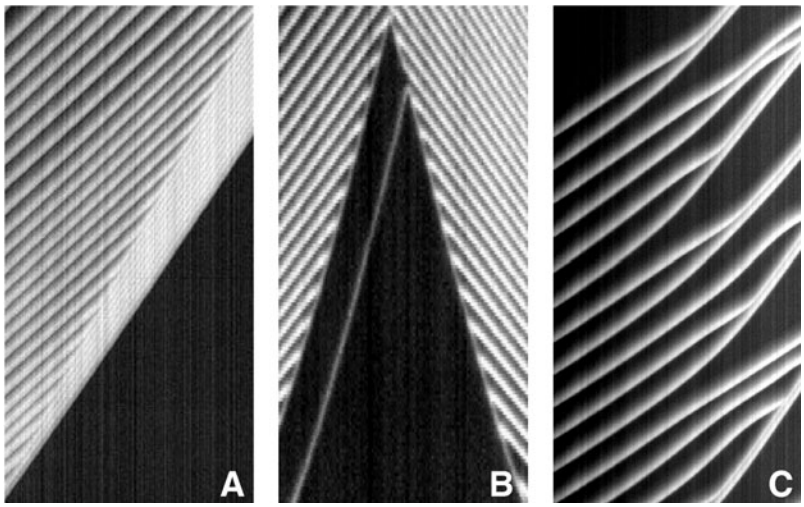


**Figure 1.** Three representative time–space plots of the wave dynamics in the 1,4-CHD–BZ reaction under pseudo-one-dimensional conditions. The horizontal space axis and the vertical time axis span 21.6 mm and 150 s in (A), 14.5 mm and 300 s in (B), and 24.7 mm and 220 s in (C), respectively. The initial concentrations are: $[H_2SO_4] = 2.0$ M (A–C), $[NaBrO_3] = 0.06$ M (A), 0.25 M (B), 0.14 M (C), [1,4-CHD] = 0.09 M (A), 0.25 M (B), 0.15 M (C), and [ferroin] = 0.5 mM (A–C).

## 3. Results

### *3.1. Quasi-one-dimensional systems*

Figure 1 illustrates the three most abundant types of behaviour observed in the CHD–BZ reaction that we refer to as stacking (A), merging (B) and bunching (C). Within these images, time evolves in an upward direction and the horizontal axis corresponds to the one spatial dimension of the reaction system. The rest state of the reaction medium is chemically reduced (i.e. $[Fe(phen)_3^{2+}] \gg [Fe(phen)_3^{3+}]$) and represented by dark areas. Each excitation pulse appears as a white band indicating a propagating transition into the oxidized state and a trailing transition back into the rest state. Accordingly, the velocity of a pulse is given by the inverse slope of the corresponding white band.

The three cases depicted in figure 1 share the common feature that excitation pulses propagate fast if the distance to their predecessor is small, whereas large distances induce low pulse speeds. This observation indicates that the corresponding dispersion curves are either fully or at least partially anomalous (i.e. $dc/d\lambda < 0$). Moreover, the first pulse traverses the system at the slowest possible speed. Consequently, all other excitation fronts decrease the distance to this first pulse in a more or less rapid fashion. This phenomenon induces front-to-back encounters that in figure 1(A) give rise to a closely stacked and expanding wavepacket. Nonetheless, each original pulse is preserved in these dense structures. As shown in figure 1(B), front-to-back encounters can also lead to the annihilation of the trailing pulses. Based on the visual appearance of the corresponding time–space plot, we refer to this process as wave merging. A detailed analysis of the underlying dispersion curves has been reported in [33] and is schematically reproduced in figure 2.

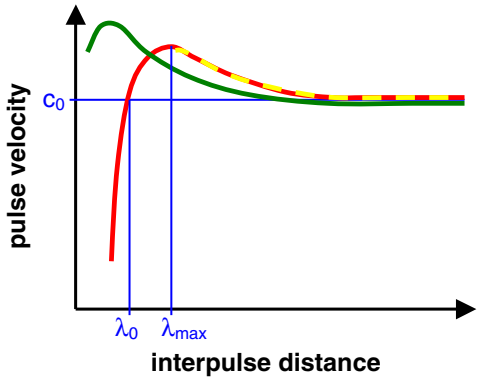


**Figure 2.** Schematic drawing of the dispersion relations that give rise to wave stacking (red), wave bunching (red/yellow) and wave merging (green).

Notice that both types of dispersion curves in figure 2 have a single maximum that separates normal from anomalous behaviour. The difference between wave stacking and merging arises from the shape of the normal segments of the curves. In the case of wave stacking, the curve falls below the speed $c_0$ for decreasing interpulse distances and hence creates a unique point $(\lambda_0, c_0)$ on the dispersion that obeys the stability criteria $\mathrm{d}c/\mathrm{d}\lambda > 0$ and $c(\lambda_0) = c_0$ [22, 23]. Under these conditions, excitation fronts can form pulse multiplets that are stable against small perturbations of their interpulse distances and in which all pulses travel with the velocity $c_0$ of the leading front. In the case of merging waves (green curve in figure 2), this attractor is not present. Here, the fast trailing pulses are moving along the dispersion curve in the direction of smaller distances until they lose stability and annihilate in a front-to-back collision with the slow leading pulse.

The scenario illustrated in figure 1(C) shows the result of an experiment in which excitation fronts cluster into pulse multiplets via a complex cascade of stacking events. The experimental parameters, and hence the underlying dispersion curve, are very similar to those in figure 1(A). However, the interpulse distance of the incoming wavefronts is large compared with the stacking pulses in figure 1(A). The bunching behaviour shown in figure 1(C) can be understood as a wave train instability in which the initially homogeneously spaced pulses rearrange to a short, stable distance and very large distances that are less unstable. This intriguing instability had not been observed earlier in any experimental system but was predicted by theoretical studies [22]–[25]. Notice that the cascade of bunching events continues until a single wavepacket is formed. An experimental analysis of this very slow process, however, is difficult because it would require unreasonably long reaction systems.

To obtain better insight into the parameter that control anomalous dispersion, we have surveyed the CHD–BZ system for a broad range of initial concentrations. Figure 3 shows a concentration space diagram in which the initial CHD and bromate concentrations are varied up to values of 0.4 and 0.25 mol $l^{-1}$ respectively. Solid red circles and blue diamonds represent systems for which no wave propagation is found. In these cases, the reaction medium remains in a reduced (i.e. red) or oxidized (i.e. blue) state respectively. These spatially homogeneous systems surround an island of initial concentration in which propagating oxidation waves are observed. These waves typically nucleate at the ends of the thin glass capillaries employed as reaction vessels. Within a band of parameters at relatively low bromate concentrations, the excitation

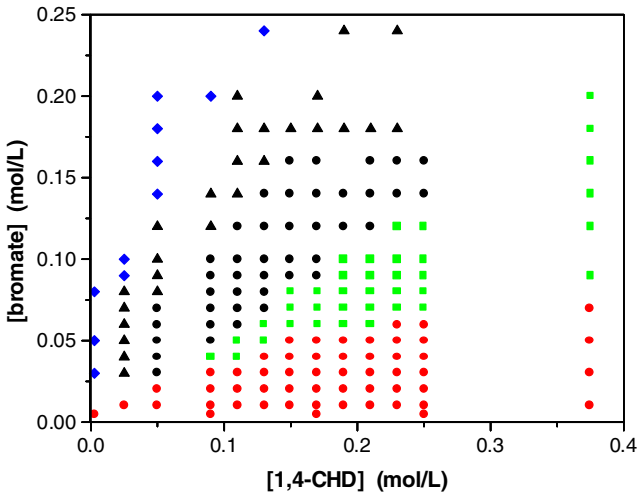


**Figure 3.** Phase diagram of the CHD–BZ reaction for sulfuric acid and ferroin concentrations of 2.0 M and 5.0 mM respectively. Red circles and blue diamonds indicate the fully reduced and oxidized media respectively. Under these conditions, no waves could be initiated. Green squares denote initial concentrations for which wave merging is observed. Black circles indicate wave stacking, whereas black triangles represent experimental conditions for which normal dispersion might exist.

waves merge similarly to those shown in figure 1(B). The corresponding initial conditions are denoted as solid green squares. At higher concentrations of sodium bromate, wave merging is replaced by wave stacking (solid black circles in figure 3). At the upper rim of the parameter island, we found no evidence for anomalous dispersion (solid black triangles). However, it should be noted that the corresponding reaction systems might reveal anomalous dispersion at very long interpulse distances that were not accessible in our experiments. In other words, their dispersion curves could resemble the one shown as a red line in figure 2 but with the maximum shifted to extremely long wavelengths.

As demonstrated by the data in figure 3, stacking and bunching of waves are widespread phenomena in the CHD–BZ reaction, whereas both phenomena are unknown in the classic BZ reaction which employs malonic acid as the organic substrate. This finding suggests that the underlying mechanisms differ from the dynamics that give rise to anomalous dispersion in two variable models such as the FitzHugh–Nagumo equations or the Tyson–Fife model [38] of the classic BZ reaction. Another unexpected finding relates to the role of the redox couple ferroin/ferriin. In the classic BZ reaction, this organometallic complex serves as a catalyst and as a convenient indicator that allows for the straightforward optical detection of the excitation waves by two-dimensional spectrophotometry. Although crucial for the formation of chemical waves, it is typically assumed that its total concentration has no or little influence on the dynamics observed. Figure 4, however, shows a pronounced dependence of the front velocity on the ferroin concentration employed.

The typical shape of the curves in figure 4 is sigmoidal and involves changes in the front velocity of a factor five or more. This dependence is possibly related to the behaviour of oscillations in well-stirred CHD–BZ systems where the complex role of ferroin has been discussed by Kurin-Csörgei *et al* [39]. It was found that the reaction behaves like a typical

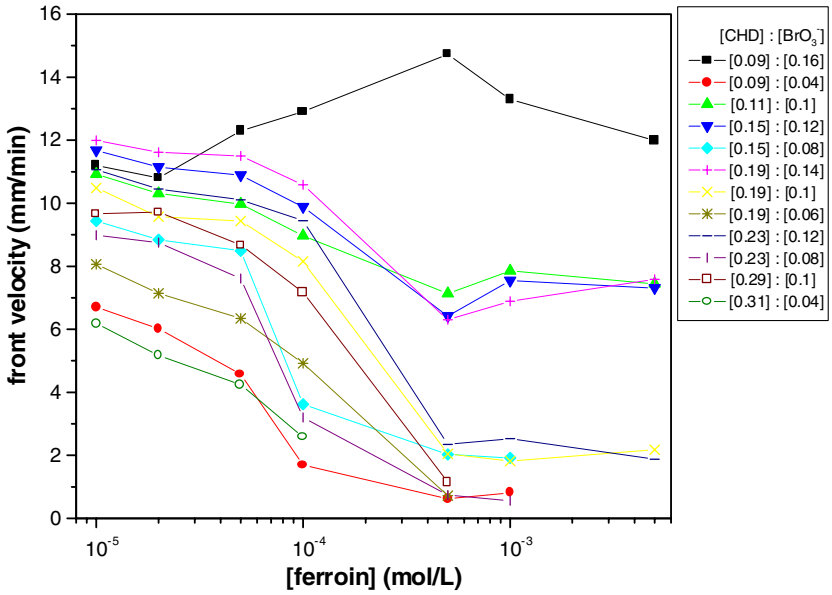


**Figure 4.** Pulse speeds as a function of initial ferroin concentration. The individual curves are measured at different initial concentrations of 1,4-cyclohexanedione and sodium bromate. The corresponding values are denoted in mol/l (see legend). The concentration of sulfuric acid is kept constant at 2.0 mol $l^{-1}$.

BZ oscillator, if the concentration of ferroin exceeds $5 \times 10^{-5}$ M. At concentrations of ferroin below $5 \times 10^{-5}$ M, however, it resembles an uncatalysed bromate oscillator (UBO). Our results (figure 4) agree well with this finding, because they reveal a marked change in the velocity of the first oxidation wave for concentrations of ferroin greater than $1 \times 10^{-4}$ M.

### *3.2. Quasi-two-dimensional systems*

The most prominent wave structures observed in two-dimensional excitable systems are rotating spiral waves and target patterns. The latter involve expanding circular fronts that nucleate from one particular pacemaker in the centre of the pattern. The pacemaker is typically a small inhomogeneity such as a dust particle or other contamination at the surface of the reaction vessel [40, 41]. To initiate waves in a periodic fashion this pacemaker must shift the reaction system from an excitable into an oscillatory state.

A representative example of a target pattern in the CHD–BZ reaction is shown in figure 5. The figure consists of three snapshots taken at intervals of 100 s. The first snapshot (A) reveals two circular wavefronts and a small oxidized spot in the centre of the pattern that eventually initiates the third front. In the subsequent frame (B), six circular fronts can be distinguished. The outermost three are closely stacked whereas the inner fronts have a relatively large interpulse distance. This behaviour is the simplest two-dimensional manifestation of the wave stacking shown in the one-dimensional case of figure 1(A). It continues in the course of the time and induces an expanding annulus of closely stacked pulses (figure 5(C)).

The stacking behaviour within the target pattern creates pronounced differences in the local excitation period. Figure 6 shows intensity traces that were extracted from a point close to the nucleation centre and from a location in the periphery of the pattern shown in figure 6. Its

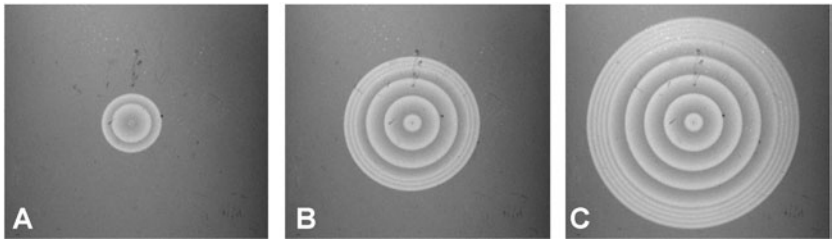


**Figure 5.** Three consecutive snapshots of a typical target pattern in the CHD–BZ reaction. The circular pulses are stacking along the outer rim of the wave pattern. Click here to see a short movie illustrating the spatio-temporal dynamics of this pattern. Time between snapshots: 100 s. Image size: 25.3 × 22.6 mm$^2$. Initial concentrations: [$NaBrO_3$] = 0.06 M, [1,4-CHD] = 0.09 M, [$H_2SO_4$] = 2.0 M, [ferroin] = 5.0 mM.

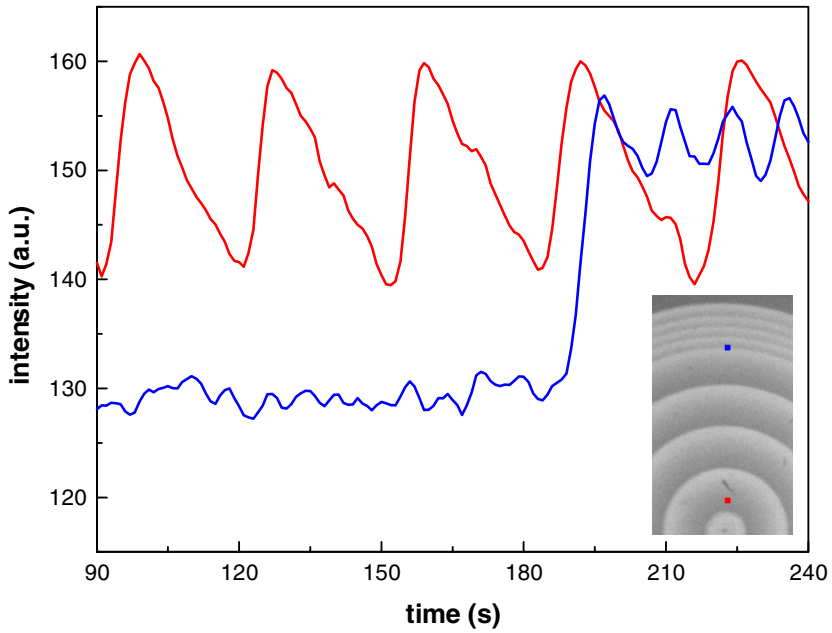


**Figure 6.** Optical intensities recorded at two different positions close to the centre (red) and in the periphery (blue) of the pattern shown in figure 5. The location of the detection points is indicated in the small inset. Their distance is 6.8 mm.

particular pacemaker generates excitation pulses with a constant period of 32 s. This period is well preserved in the red trace that is extracted from the position in close proximity to the pacemaker. At the distant point, however, the excitation period has decreased to 13 s as illustrated by the blue curve in figure 6. Notice that the latter curve is initially flat since a relatively long time (∼3 min) passes until the arrival of the first wavefront.

A surprising consequence of our observation is the existence of two dominant excitation periods within the target pattern. A given point within the pattern is either subject to the high-frequency pulses of the stacked outer rim or under the influence of the driving period of the pacemaker. The transition between this low-frequency near-field and the high frequency within

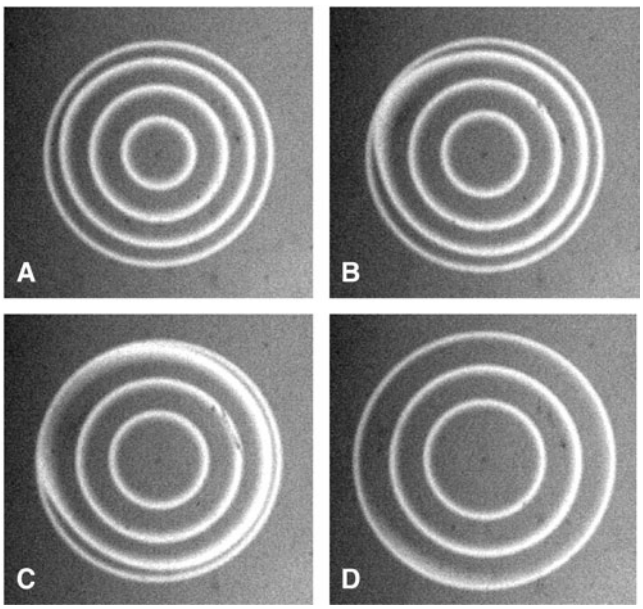


**Figure 7.** Four consecutive snapshots of a typical target pattern in the CHD–BZ reaction. The circular pulses are merging along the outer rim of the wave pattern. Click here to see a short movie illustrating the spatio-temporal dynamics of this pattern during its early stages. Time between snapshots: 10 s. Image size: $13.8 \times 13.0$ mm$^2$. Initial concentrations: [$NaBrO_3$] = 0.09 M, [1,4-CHD] = 0.19 M, [$H_2SO_4$] = 2.0 M, [ferroin] = 5.0 mM.

the stacked outer rim occurs over a relatively short distance. Accordingly, the transition region has the shape of a very thin annulus and propagates with it is own characteristic velocity. A simple analysis [34] reveals that this velocity $c_s$ is given by the two dominant speeds and periods (or interpulse distances) of the fronts within the target pattern according to the equation

$$c_s = (c_0\lambda_1 - c_1\lambda_0)/(\lambda_1 - \lambda_0) = c_0c_1(T_1 - T_0)/(c_1T_1 - c_0T_0),$$

where $c_i$, $\lambda_i$ and $T_i$ ($i = 0, 1$) denote the speed, interpulse distance and period of the leading pulse ($i = 0$) and the fast, inner fronts ($i = 1$) respectively.

Figure 6 reveals an additional feature of excitation waves in the CHD–BZ reaction. The intensity changes reflect the oxidation state of the catalyst which is the only chemical species that absorbs visible light in this reaction system. High intensity values indicate that a large fraction of the catalyst is oxidized whereas low values correspond to the chemically reduced state. The data presented in figure 6 reveal that neither the high frequency nor the low frequency pulses recover the oxidation characteristics of the reduced rest state. Furthermore, the intensity decay in the wake of the pulses shows no overshot or damped oscillations. Hence, we are able to conclude that the oxidized catalyst (ferriin) is not the control variable that induces anomalous dispersion although it might participate in the overall dynamics.

We also probed various pseudo-two-dimensional CHD–BZ systems for the existence of target patterns that undergo wave merging. Our experiments revealed that these exotic structures indeed exist and that the chemical conditions for their formation can be predicted from the phase diagram shown in figure 3. Figure 7 shows a typical example of such a merging target pattern. The four snapshots illustrate the dynamics of the target pattern during a relatively late stage.

These data are accompanied by a movie that has been compiled from frames obtained during earlier stages of the evolution of the same pattern. The snapshots as well as the movie reveal that the outermost front propagates at a relatively low velocity and that the subsequent, fast pulses annihilate with it in front-to-back collisions. Accordingly, this behaviour is analogous to the one-dimensional merging dynamics shown in figure 1(B).

Despite this analogy of one- and two-dimensional systems, figure 7 also reveals an interesting feature that is either absent or less readily observed in the one-dimensional case. While snapshots (A) and (D) show a target pattern of nearly perfect circular symmetry, pronounced deviations are apparent during the close encounter of the second outermost front with the leading pulse (B), (C). In the ten o'clock direction, the trailing pulse reaches its predecessor early and induces a striking deformation from the initial circular front shape. We suggest that this phenomenon is due to the amplification of small initial perturbations in the nonlinear velocity field created by the leading pulse. These initial perturbations might be partially induced by anomalous behaviour in the near vicinity of the pacemaker which seems to nucleate pulses in a slightly asymmetric fashion.

## 4. Conclusions

In summary, this study presents experimental results that illustrate some of the most pertinent differences between the CHD–BZ and the classic BZ reaction. Whereas wave propagation in the latter system is governed by normal dispersion relations, the CHD–BZ reaction shows an abundance of phenomena that are characteristic for anomalous dispersion. These include the formation of closely stacked wavepackets that are observed in one- as well as two-dimensional systems.

An intriguing feature of these wavepackets is that they are expected to be stable against perturbations. In other words, externally induced variations of their characteristic interpulse distance will decrease rapidly to re-establish the original configuration. Large distances between individual wavepackets are only mildly unstable, meaning that their fusion would require extremely long times. From a practical point of view, this opens up fascinating possibilities for their use in signal transmission. For example, one can envision the encoding of information in terms of the number of individual pulses constituting a particular wavepacket. Sequences of these packets could then relay information over large distances in the form of information blocks that are stable against perturbations.

While the authors do not expect any immediate technical developments to arise from anomalous excitation waves, it is tempting to speculate about their relevance in biological systems. Waves of action potential in neuronal systems can be subject to dispersion phenomena that are similar to those discussed in this work [29, 42]. This behaviour is often referred to as supernormal excitability [43] and it might affect the operation of neuronal networks in unexpected ways.

Also many open questions remain in the context of the CHD–BZ reaction. Our data show that anomalous dispersion is more abundant than expected from the simple two-species models discussed in the introduction. This finding suggests that anomalous dispersion arises from a specific feature of the underlying reaction mechanism. For example, the relaxation dynamics in the wake of an excitation pulse could be controlled by two or more chemical species such as an activator and an inhibitor that change concentration levels with different rates and hence create an 'optimal' distance for a subsequent pulse. This suggestion is also supported by our

finding that the concentration of ferriin decreases monotonically in the wake of pulse without any overshoots or ripples.

In conclusion, we believe that the CHD–BZ reaction is an ideal model for further investigations of excitable systems with anomalous dispersion. While this study presented some insights into the dynamics of simple two-dimensional target patterns, more work is needed to explore the intricate balance between anomalous pulse propagation and curvature-induced velocity changes [44]. In particular, it will be interesting to study the dynamics of wave collisions in front-to-front encounters and the dynamics of spiral wave rotation.

## Acknowledgment

This work was supported by the National Science Foundation (NSF grant CHE-20023105).

## References

[1] Epstein I R and Pojman J A 1998 *An Introduction to Nonlinear Chemical Dynamics* (New York: Oxford University Press)
[2] Kapral R and Showalter K (ed) 1995 *Chemical Waves and Patterns* ( Dordrecht: Kluwer)
[3] Dolnik M, Berenstein I, Zhabotinsky A M and Epstein I R 2001 *Phys. Rev. Lett.* **87** 238301
[4] Niedernostheide F J, Arps M, Dohmen R, Willebrand H and Purwins H G 1992 *Phys. Status Solidi* b **172** 249
[5] Sakurai T, Mihaliuk E, Chirila F and Showalter K 2002 *Science* **296** 2009
[6] Müller S C, Mair T and Steinbock O 1998 *Biophys. Chem.* **72** 37
[7] Merzhanov A G and Rumanov E N 1999 *Rev. Mod. Phys.* **71** 1173
[8] Lechleiter J, Girard S, Peralta E and Clapham D 1991 *Science* **252** 123
[9] Steinbock O, Hashimoto H and Müller S C 1991 *Physica* D **48** 233
[10] Witkowski F X, Leon L J, Penkoske P A, Giles W R, Spano M L, Ditto W L and Winfree A T 1998 *Nature* **392** 78
[11] Dahlem M A and Müller S C 1997 *Exp. Brain Res.* **115** 319
[12] Ross J, Müller S C and Vidal C 1988 *Science* **240** 460
[13] Gierer A and Meinhard H 1972 *Kybernetik* **12** 30
[14] Field R J and Burger M (ed) 1985 *Oscillations and Travelling Waves in Chemical Systems* (New York: Wiley)
[15] Steinbock O and Müller S C 1992 *Physica* A **188** 61
[16] Winfree A T 1991 *Chaos* **1** 303
[17] Dockery J D, Keener J P and Tyson J J 1988 *Physica* D **30** 177
[18] Pagola A, Ross J and Vidal C 1988 *J. Phys. Chem.* **92** 163
[19] Nassar S F, Ismail H A, Sayed E M and El-Falaky A 1975 *Appl. Phys.* **7** 307
[20] Siegert F and Weijer C 1989 *J. Cell Sci.* **93** 325
[21] Flesselles J M, Belmonte A and Gaspar V 1998 *J. Chem. Soc. Faraday Trans.* **94** 851
[22] Rinzel J and Maginu K 1984 *Non-equilibrium Dynamics in Chemical Systems* ed C Vidal and A Pacault (Berlin: Springer) pp 107–13
[23] Elphick C, Meron E and Spiegel E A 1988 *Phys. Rev. Lett.* **61** 496
[24] Elphick C, Meron E and Spiegel E A 1990 *SIAM J. Appl. Math.* **50** 490
[25] Elphick C, Meron E, Rinzel J and Spiegel E A 1990 *J. Theor. Biol.* **146** 249
[26] Or-Guil M, Kevrekidis I G and Bär M 2000 *Physica* D **135** 154
[27] Winfree A T 1990 *Phys. Lett.* **149** 203
[28] Winfree A T 1991 *Physica* D **49** 125
[29] Goldermann M, Hanke W, Guimaraes De Almeida A C and Fernandes De Lima V M 1998 *Int. J. Bifurcation Chaos* **8** 1541

[30] Siegert F and Weijer C J 1991 *Physica* D **49** 224
[31] Christoph J, Eiswirth M, Hartmann N, Imbihl R, Kevrekidis I and Bär M 1999 *Phys. Rev. Lett.* **82** 1586
[32] Manz N, Müller S C and Steinbock O 2000 *J. Phys. Chem.* A **104** 5895
[33] Hamik C T, Manz N and Steinbock O 2001 *J. Phys. Chem.* A **105** 6144
[34] Hamik C T and Steinbock O 2002 *Phys. Rev.* E **65** 046224
[35] Kurin-Csörgei K, Zhabotinsky A M, Orban M and Epstein I R 1997 *J. Phys. Chem.* A **101** 6827
[36] Davydov V A, Manz N, Steinbock O, Zykov V S and Müller S C 2000 *Phys. Rev. Lett.* **85** 868
[37] Davydov V A, Manz N, Steinbock O and Müller S C 2002 *Europhys. Lett.* **59** 344
[38] Tyson J J and Fife P C 1980 *J. Chem. Phys.* **73** 2224
[39] Kurin-Csörgei K, Zhabotinsky A M, Orban M and Epstein I R 1996 *J. Phys. Chem.* **100** 5393
[40] Nagashima H 1991 *J. Phys. Soc. Japan* **60** 2797
[41] Bugrim A E, Dolnik M, Zhabotinsky A M and Epstein I R 1996 *J. Phys. Chem.* **100** 19017
[42] Brenner N, Agam O, Bialek W, de Ruyter van Steveninck R R 1998 *Phys. Rev. Lett.* **81** 4000
[43] Bartesaghi R 1987 *Exp. Neurol.* **96** 208
[44] Steinbock O 2002 *Phys. Rev. Lett.* **88** 228302